

BAYESIAN ERROR PROPAGATION FOR NEURAL-NET BASED PARAMETER INFERENCE

DANIELA GRANDÓN

Grupo de Cosmología y Astrofísica Teórica, Departamento de Física, FCFM, Universidad de Chile, Blanco Encalada 2008, Santiago, Chile.

Mathematical Institute, Leiden University, Snellius Gebouw, Niels Bohrweg 1, NL-2333 CA Leiden, The Netherlands.

ELENA SELLENTIN

Mathematical Institute, Leiden University, Snellius Gebouw, Niels Bohrweg 1, NL-2333 CA Leiden, The Netherlands.
 Leiden Observatory, Leiden University, Oort Gebouw, Niels Bohrweg 2, NL-2333 CA Leiden, The Netherlands.

Version May 25, 2022

ABSTRACT

Neural nets have become popular to accelerate parameter inferences, especially for the upcoming generation of galaxy surveys in cosmology. As neural nets are approximative by nature, a recurrent question has been how to propagate the neural net's approximation error, in order to avoid biases in the parameter inference. We present a Bayesian solution to propagating a neural net's approximation error and thereby debiasing parameter inference. We exploit that a neural net reports its approximation errors during the validation phase. We capture the thus reported approximation errors via the highest-order summary statistics, allowing us to eliminate the neural net's bias during inference, and propagating its uncertainties. We demonstrate that our method is quickly implemented and successfully infers parameters even for strongly biased neural nets. In summary, our method provides the missing element to judge the accuracy of a posterior if it cannot be computed based on an infinitely accurately theory code.

1. INTRODUCTION

Cosmology currently finds itself in the fortunate state of collecting ever more, and in particular ever more precise data. The science-ready data sets of the upcoming surveys are forecasted to contain multiple million data points, yielding sub-percent precision on many cosmological parameters (Laureijs et al. 2011; LSST Science Collaboration et al. 2009; Mellema et al. 2013). Likewise, the trend of collecting vaster, more precise data, is repeated in all other disciplines of astronomy that equally enjoy a progress in instrumentation.

If physical models and parameters are to be inferred from such data, then the increasing precision of data demands an equal increase in the precision of theoretical models. This need for improved theoretical modelling invalidates the formerly seen use of fast approximations, often resulting in numerical challenges that range from demanding to prohibitive. As artificial neural nets are – once trained – compellingly fast, astronomy lately sees a surge of neural-net based emulation of theoretical models and likelihoods.

Manrique-Yus & Sellentin (2020) provide neural net predictions for half a million data points of a Euclid-like survey, computing the posterior of seven cosmological parameters when also emulating the theoretical predictions for a Planck-like (Planck Collaboration 2018) observation of the cosmic microwave background. Sperio Mancini et al. (2022) provide a neural net emulator of the cosmic matter powerspectrum, which facilitates the incorporation of nuisance parameters. In de Mijolla et al. (2019), the authors provide neural net based molecular line modelling for inferences in astrochemistry. Neural

net based inference has also been demonstrated on simulated LSST-year1 data in Boruah et al. (2022).

Common to all of these examples is that the respective authors demonstrate the validity of their neural-net based inference by comparing to the posterior computed with a classical non-approximative code. In an actual research case, this comparison will often be unfeasible: if the neural-net assisted posterior is the only one that can be computed in reasonable time, then no other posterior is available for comparison. It would then be uncertain whether the neural net had the required accuracy to enable an unbiased inference.

Accordingly, a thus far unsolved problem in neural-net assisted inference was how to avoid that the neural net's approximation error will bias the parameter inference. As any neural net is by setup an approximator, it is vital to have a clean solution for propagating its error.

This paper hence presents an adapted posterior function, which is the Bayesian solution to the wish of wanting to eliminate a neural net's bias and propagating the uncertainty of its prediction. Crucially, our solution is expected to work for a wide range of successfully and rather unsuccessfully trained neural nets. As the neural net training improves, our adapted posterior converges to the posterior yielded by traditional non-neural net based inferences.

Our paper is structured as follows. The Bayesian solution to propagating biases and approximation errors in a neural-net assisted inference is presented in Sect. 2. This papers' main result are Eq. (7) and Eq. (8), which give the adapted posterior function that replaces the posterior yielded from a non-approximate code. Eq. (7) is the special case of Eq. (1) if the data follow a Gaussian sampling distribution and the neural net's errors can be approximated as Gaussian too. Sect. 3 compares this

adapted posterior to the ‘naive’ posterior gained from wrongly assuming the neural net has an infinite precision. We demonstrate two cases of varying neural net training success. Our results are briefly discussed in Sect. 4.

2. BAYESIAN POSTERIOR FOR NEURAL-NET ASSISTED INFERENCE

We assume a neural net that has been trained to output predictions $\mu_{\text{NN}}(\mathbf{p})$, and has undergone validation by testing its predictions on an independent validation set that contains V samples of parameters \mathbf{p} .

The neural net’s approximation error can then be evaluated at each sample of this validation set, and we define the discrepancy between the neural net prediction and the original mean of the likelihood to be $\Delta(\mathbf{p}) = \mu(\mathbf{p}) - \mu_{\text{NN}}(\mathbf{p})$. However, in the space between the validation points, the approximation error will remain unknown. Hence, as $\Delta(\mathbf{p})$ is unknown for all but a few points in parameter space, we promote it to a random, since uncertain, variable in the Bayesian sense. We shall therefore treat $\Delta(\mathbf{p})$ as random for the same reason that the unknown covariance matrix of Sellentin & Heavens (2016) is treated as random.

For any random variable, a Bayesian solution requires the probability distribution that this variable follows. We denote the distribution as $\Delta(\mathbf{p}) \sim \mathcal{D}(\Delta(\mathbf{p})|\cdot)$, where the placeholder \cdot denotes variables that specify the distribution further, for example, a mean and a variance if \mathcal{D} is a Gaussian.

In the worst case of neural net training, the neural net will have approximation errors that strongly vary with the values of \mathbf{p} . For example there might be parameter ranges for which the neural net succeeds in approximating the parametric explanation of the data, and there might be areas where it deviates strongly from the training set. In this case, we would have $\mathcal{D}(\Delta(\mathbf{p})|\mathbf{p}, \cdot)$, i.e. the distribution of neural net approximation errors will explicitly depend on the parameters themselves. A Bayesian solution to propagating the neural net’s errors would then still be possible, as long as \mathcal{D} can be accurately estimated. This could e.g. be achieved by histogramming the approximation errors over different patches of the parameter range. Another solution to a spatially-varying distribution \mathcal{D} would be to model it with a Gaussian process, see e.g. Mootoovaloo et al. (2020), who however find that propagating a full Gaussian process error is too complex, resulting in a posterior that is worse than if the approximation error were ignored.

Adopting a Gaussian process would also allow us to treat the approximation error as known at all validation points. However, using a Gaussian process for the sake of modelling spatially varying approximation errors necessitates that hyperparameters must be set. To avoid such hyper-parameters, we hence prefer to treat the approximation error as random also at the validation points. This is a conservative choice as it treats the approximation error at the validation points with the same uncertainty as in between the validation points.

We hence adopt the approximation that for all values of \mathbf{p} , the neural net’s errors follow the same distribution, namely $\Delta \sim \mathcal{D}(\Delta|\cdot)$, where the placeholder \cdot now excludes the parameters \mathbf{p} . This working hypothesis could be dropped at the expense of a more involved derivation,

but in numerical experiments of reasonably trained nets we found it to hold with excellent precision.

2.1. Marginalizing the neural net error and bias

We assume the neural net provides parametric predictions for n data points, and we denote the scientific data by \mathbf{x} ¹. The likelihood of the data $\mathcal{L}(\mathbf{x}|\mathbf{p}, \Delta)$ is dependent on the neural net’s approximation error Δ : if the neural net’s prediction is erroneous, other values of the parameters \mathbf{p} might fit the data better in order to compensate for the neural net’s error. Such a bias in the inferred parameters is the key worry we here aim to eliminate by accounting for the neural net’s error.

We also assume that the prior probability of the parameters $\pi(\mathbf{p})$ is independent of the prior probability of approximation errors $\pi(\Delta)$. This will hold if the neural net was trained according to best practice. Nonetheless, counterexamples can be engineered, namely when the neural was trained on highly unrepresentative samples of \mathbf{p} .

Propagating the neural net’s prediction error then implies that we must marginalize Δ . The posterior of parameters inferred from an imperfect neural net prediction is hence the compound of the posterior of vanishing neural net error with the distribution of the error

$$\begin{aligned} \mathcal{P}(\mathbf{p}|\mathbf{x}) &= \int \mathcal{P}(\mathbf{p}, \Delta|\mathbf{x}) d^n \Delta \\ &= \int_{-\infty}^{+\infty} \mathcal{P}(\mathbf{p}|\Delta, \mathbf{x}) \mathcal{D}(\Delta|\cdot) d^n \Delta \\ &\propto \int_{-\infty}^{+\infty} \mathcal{L}(\mathbf{x}|\mathbf{p}, \Delta) \pi(\mathbf{p}) \mathcal{D}(\Delta|\cdot) d^n \Delta, \end{aligned} \quad (1)$$

where the proportionality sign arises by not having written out the normalization with the Bayesian evidence.

Eq. (1) describes that parameter inference can be safeguarded against a neural net’s approximation error by specifying the data’s likelihood as a function of physical parameters and the net’s approximation error, setting a prior on the parameters, and compounding with the distribution of the net’s approximation error. The posterior of physical parameters is hence the marginal over the neural net’s approximation error.

We shall now specialize Eq. (1) to the most common case of Gaussian data.

2.2. Specialization to Gaussian data

In this section we provide a closed-form expression for the posterior of marginalized neural net error for the case of Gaussianly distributed data.

In line with this assumption, the likelihood now reads

$$\mathcal{L}(\mathbf{x}|\mathbf{p}) \propto \exp\left(-\frac{1}{2}[\mathbf{x} - \mu(\mathbf{p})]^T \mathbf{C}^{-1} [\mathbf{x} - \mu(\mathbf{p})]\right), \quad (2)$$

where μ is the error-free mean of the data, evaluated as a function of the parameters \mathbf{p} , and \mathbf{C}^{-1} is the inverse covariance matrix of the data.

Defining $\xi(\mathbf{p}) = \mathbf{x} - \mu(\mathbf{p})$, the likelihood with neural

¹ The scientific data are not the training set.

net error is

$$\mathcal{L}(\mathbf{x}|\mathbf{p}, \Delta) \propto \exp\left(-\frac{1}{2}[\xi(\mathbf{p}) - \Delta]^T C^{-1}[\xi(\mathbf{p}) - \Delta]\right). \quad (3)$$

We define the mean of the neural net approximation error as

$$\bar{\Delta} = \frac{1}{V} \sum_{v=1}^V \Delta_v \quad (4)$$

were v runs over the samples of the validation set. Accordingly, the covariance matrix of the neural net's prediction error is

$$\Sigma = \frac{1}{V-1} \sum_{v=1}^V (\Delta_v - \bar{\Delta})(\Delta_v - \bar{\Delta})^T. \quad (5)$$

For an excellently trained neural net, the mean $\bar{\Delta}$ will vanish, meaning the neural net provides an unbiased prediction of the theory function over the entire parameter range. On the other hand, the covariance matrix Σ will contain large variances and covariances for a neural net whose training did not yield very accurate predictions of the target function. The more training samples were seen, and the smaller the loss during training, the smaller the elements of Σ will become. The Gaussian distribution of Δ then is

$$\mathcal{D}(\Delta) \propto \exp\left(-\frac{1}{2}[\Delta - \bar{\Delta}]^T \Sigma^{-1}[\Delta - \bar{\Delta}]\right). \quad (6)$$

In the limit $\Sigma \rightarrow 0$, this distribution tends to Dirac's delta distribution, correctly reflecting that no errors are folded into the posterior of parameters.

As the compound of a Gaussian with another Gaussian yields a third Gaussian, inserting Eq. (3) and Eq. (6) into Eq. (1) yields

$$\mathcal{P}(\mathbf{p}|\mathbf{x}) \propto \exp\left(-\frac{1}{2}[\xi(\mathbf{p}) - \bar{\Delta}]^T \Psi[\xi(\mathbf{p}) - \bar{\Delta}]\right) \pi(\mathbf{p}), \quad (7)$$

where

$$\Psi = (C + \Sigma)^{-1}, \quad (8)$$

and $\bar{\Delta}$ is given by Eq. (4). We expect Eq. (7) to be the result of this paper that is at minimum effort most widely applicable: For a neural net that produces approximately Gaussian distributed inaccuracies in its predictions, Eq. (7) propagates the net's uncertainties, and eliminates the net's bias due to the subtraction of $\bar{\Delta}$. Eq. (7) hence eliminates neural net biases in the inference of cosmological parameters.

3. DEMONSTRATION OF PARAMETER INFERENCE

In this section we demonstrate the inference of parameters when the theory prediction for the data has been computed with a neural net. We will highlight two cases of how (un)successful neural net training deforms the posterior of inferred parameters.

For our demonstration, we simulated a cosmological analysis of the matter power spectrum $P(k)$ as a function of wavenumber k . Our data range spans $k \in [0.0033, 0.4]$ in units of h/Mpc . In order to train a neural net, we generate 10000 power spectra with CAMB [Lewis & Bridle](#)

	Prior ranges	Fiducial cosmology
Ω_{cdm}	[0.22,0.4]	0.269
Ω_b	[0.02,0.06]	0.0494
H_0	[58,82]	66.8

TABLE 1: Prior ranges and input cosmology for Ω_{cdm} , Ω_b and H_0 .

([2002](#)) by randomly drawing from the prior ranges given in Table 1 for the parameters H_0 , Ω_{cdm} , Ω_b , which are the Hubble constant, the density parameter of cold dark matter, and the density parameter of baryons, respectively. We split the CAMB predictions into a batch of 70% for training, 20% for the validation set and 10% for test. We also segmented the power spectra into wavenumber ranges of $k \in [0.0033, 0.044]$ and $k \in [0.044, 0.40]$ and trained a neural net for each k -range individually. The segmentation into k -ranges is not necessary, but advantageous because it reduces the layer sizes and thereby the trainable parameters.

For the training we engineered two cases. One is a successfully/accurately trained neural net whose error on the test set is at the percent level on average over k . The second case is an unsuccessfully/inaccurately trained neural net where the prediction error is up to 40%. Such big an error would clearly bias the posterior of cosmological parameters unless it is corrected for. Further details about the performance of our neural nets are presented in Appendix A.

We test the performance of the two neural nets on a new validation set \mathbf{V} including new 10000 power spectra at random \mathbf{p} from the prior range. For each point v in \mathbf{V} it is possible to obtain the neural net approximation error $\Delta_v(\mathbf{p}) = \mu(\mathbf{p}) - \mu_{\text{NN}}(\mathbf{p})$ that accounts for the bias in the prediction, and v runs from 1 to 10000.

In this paper, as stated in Section 2.2, we assume Δ is a random variable that follows a Gaussian distribution, so it is crucial to check this assumption by computing histograms for different k . Fig.1 shows histograms for the two models at different k . As a very basic test, the mean and the median are displayed as we expect both match for a normally distributed sample. We also computed skewness and curtosis and ensured that no bimodal structure occurs in the histograms. We found that our assumption of Gaussianity is indeed supported.

For both upper and lower panels of Fig. (1), the first two figures from left to right show cases where gaussianity assumption is completely fulfilled. The third column shows handpicked examples where the gaussian approximation is stretched, but is a very rare case and no more extreme cases were observed.

As presented in Eq. (7), our adapted posterior accounts for the bias and the appoximation error by defining $\bar{\Delta}$ and Σ . From $\Delta_v(\mathbf{p})$, we apply Eq. (4) and Eq. (5) to obtain $\bar{\Delta}_{\text{acc}}, \Sigma_{\text{acc}}$ and $\bar{\Delta}_{\text{inacc}}, \Sigma_{\text{inacc}}$ for the accurate and inaccurate models, respectively. The prediction errors $\bar{\Delta}_{\text{acc}}$ and $\bar{\Delta}_{\text{inacc}}$ are displayed in Fig. 2, and compared to the power spectra at the input cosmology. The Lower panel shows the fractional difference that goes up to 5% compared to the input power spectra for the accurate neural net, and 40% for the inaccurate model. Hence, we expect the bias of the best fit of parameters is negligible when comparing the resulting posteriors with and

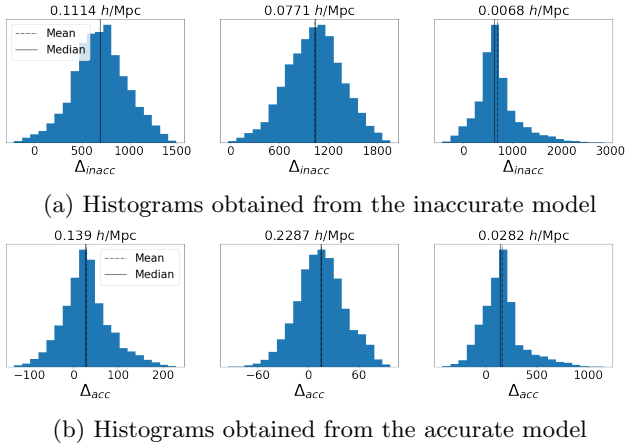


FIG. 1.—: Histograms of Δ at specific wave number k obtained for all the points in the validation set. From left to right, the two first histograms represent the general tendency of our histograms, where gaussianity condition is fullfilled. The third column shows histograms where the distributions slightly deviate from gaussianity.

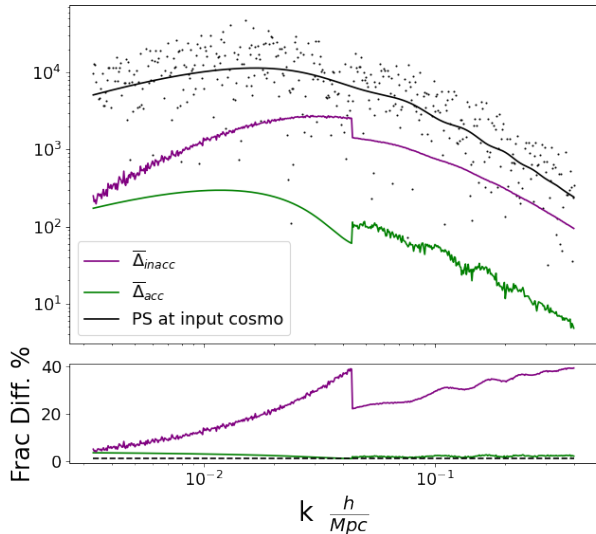


FIG. 2.—: The prediction errors for the two neural nets are displayed and compared to the matter power spectra at the input cosmology. The prediction error for the accurate model Δ_{acc} is shown in green and the prediction error Δ_{inacc} for the inaccurate model in purple. The scatter plot represent the synthetic matter power spectra used for the inference.

without error propagation. In Fig. 3 we see the variance and covariances for the unsuccessfully trained model are larger, hence impacting strongly the covariance matrix of the adapted posterior.

Once all the components of Eq. (7) are derived, we constrain cosmological parameters for three scenarios: when the theory prediction is computed by CAMB, and when the prediction is done with the accurate neural net model, and inaccurate model. Moreover, for neural-net based inference we consider the cases when the posterior

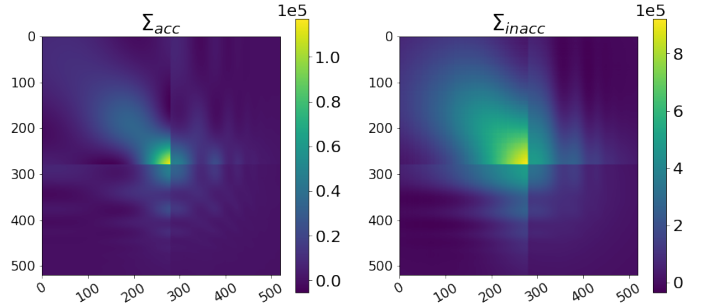


FIG. 3.—: Left: the covariance matrix Σ_{acc} . Right: Σ_{inacc} . We see that the badly trained neural net causes not only a higher bias as seen in Fig. (2) but additionally also more correlated errors in its prediction.

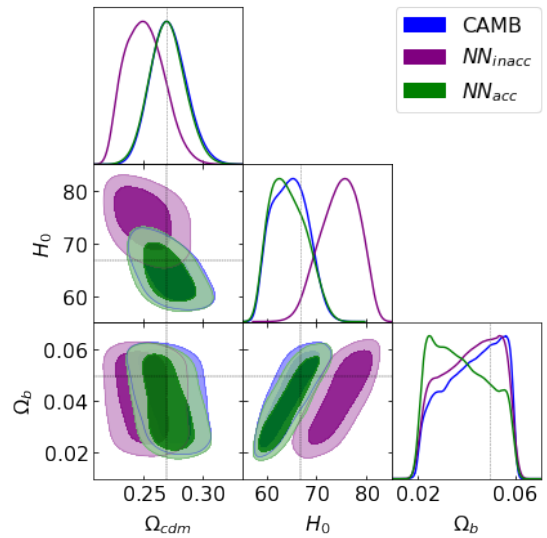


FIG. 4.—: Marginal posterior contours obtained for neural-net based inference and normal Boltzmann-code based inference for synthetic matter power spectra data. The contours contain 68% and 90% posterior volume.

does and does not propagate the neural net’s error, where the former is the adapted posterior proposed in Eq. (7) and the latter a naive plug-in of the neural net into the standard Gaussian likelihood.

We generated synthetic matter power spectra by Gaussian random draw from a mean, depending on input parameters $H_0 = 66.8$, $\Omega_{\text{cdm}} = 0.269$, $\Omega_b = 0.0494$, and a covariance matrix \mathbf{C} as the square of the fiducial power spectrum. The mean is displayed as a black solid line in Fig. 2, where the synthetic data scatters around.

In all figures, purple contours stand for the posteriors obtained from the inaccurate neural net, and green posteriors for the accurate net. The input parameters are indicated in all corner plots by dashed black lines. In Fig. 4, we depict the ‘naive’ posteriors, yielded by simply replacing the (taken as infinitely accurate) CAMB mean $\mu(\mathbf{p})$ with the neural net’s prediction, neither propagating the neural net’s bias nor its approximation error around the true mean. Purple contour show a noticeable non-zero bias in the best fit, while the green contour mostly match the CAMB blue contour. Hence, Fig. 4

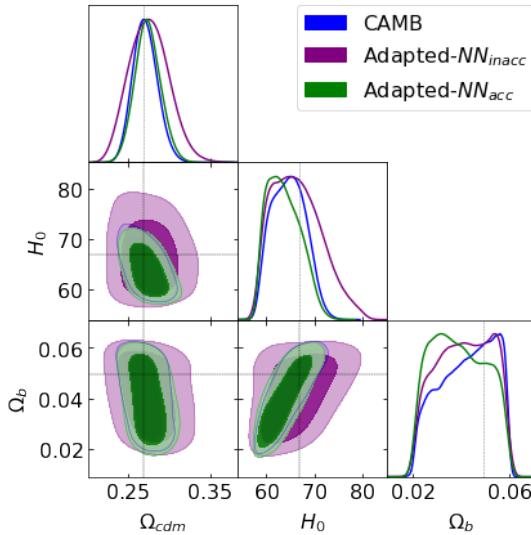


FIG. 5.—: Marginal posterior contours obtained for neural-net based inference implementing the proposed adapted posterior. CAMB results are also displayed for comparison. The contours contain 68% and 90% posterior volume.

demonstrates that parameter inference will incur biases if the neural net's approximation error is not propagated.

Accordingly, Fig. 5 demonstrates the main results of this work, namely the adapted-posterior that propagates the neural nets errors into the final parameter inference. For both neural nets, the posterior of parameters is widened up due to the neural nets approximation error. This is a consequence of the covariance matrix of the neural net approximation error shown in Fig. 3. As this covariance matrix adds to the original covariance matrix of the data, the uncertainty on the parameter constraints increases. This is much more prominent for the inaccurately trained neural net. Also seen is that the subtraction of the neural net's bias leads to a debiasing of the posterior: The fiducial cosmology is included in the posterior after debiasing, but is excluded beforehand. This evidences that our Eq. (7) is a simple but powerful method for safeguarding parameter inference against the approximative nature of neural nets.

4. DISCUSSION

In this work we derived an adapted posterior that propagates the error of the theory predictions of neural-net based inference. The adapted posterior results in Eq. 7 and 8, and implies a modified precision matrix and a bias correction when the error in the neural net prediction is non-negligible. We investigate the impact of the neural net prediction error on a cosmological analysis for constraining parameters Ω_{cdm} , Ω_b and H_0 . The method is easy to implement when the prediction errors follow a gaussian distribution, which must be checked. It is worth noting that for this approximation gaussianity holds even if a few examples present mild longer tails. However, non-negligible higher moments can emerge in cases where the distribution is bimodal or where heavy tails are present. In those cases it is crucial to either extend the analysis and propose a new analytic form for

$\mathcal{D}(\Delta)$, or to improve the neural net training, in order to achieve Gaussian approximation errors. In this analysis,

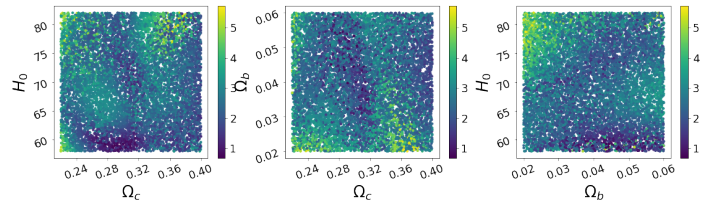


FIG. 6.—: Scatter plot of parameter space where the colorbar stands for the average (over all wave numbers) percentage error in the prediction made by the accurate neural net.

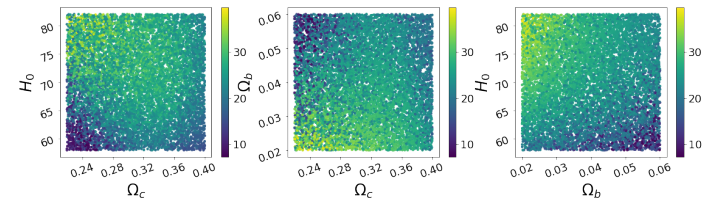


FIG. 7.—: Same as Fig. (6) but for the inaccurate neural net.

we found that gaussianity holds in most of the trained models, making the method simple to apply.

In Section 3 we show that error propagation can restore the input cosmology in the best-fit even if the neural net is inaccurate.

As many works in the literature had shown the advantages of accelerated neural-net based inference in the context of future Stage-IV cosmological surveys, we consider it critical to also include error propagation for neural nets inference. In the era of precision cosmology, where many efforts are still being done on the control of astrophysical or instrumentation systematic effects, it is also necessary to consider and characterise the biases that our modern statistical methods propagates into the inference.

ACKNOWLEDGEMENTS

We thank the support staff of Leiden's ALICE High Performance Computing infrastructure. DG acknowledges financial support by project ANIDPFCHA/Doctorado Nacional/2019-2119188 and thanks the Mathematical Institute of Leiden University for the hospitality during this research.

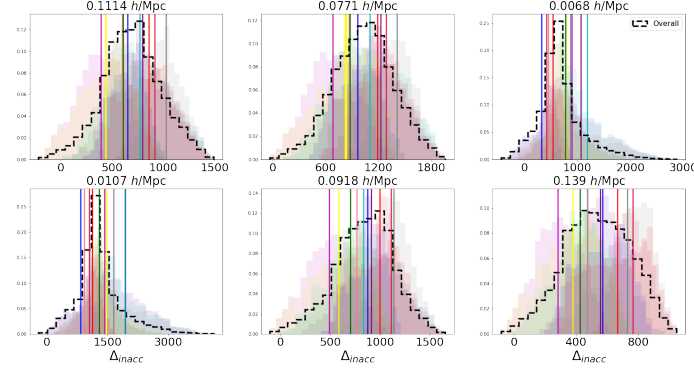


FIG. 8.—: Sub-volume histograms for different wavenumber k , where Δ is obtained with the inaccurate neural net. The overall distribution over all parameter space is depicted in a dashed-black contour. Shaded colors in the background represent the obtained histograms for different chosen sub-volumes, where the means are shown in vertical coloured lines. We conclude that the neural net approximation error does not directly depend on the sub-volume and hence not directly on the cosmological parameters themselves.

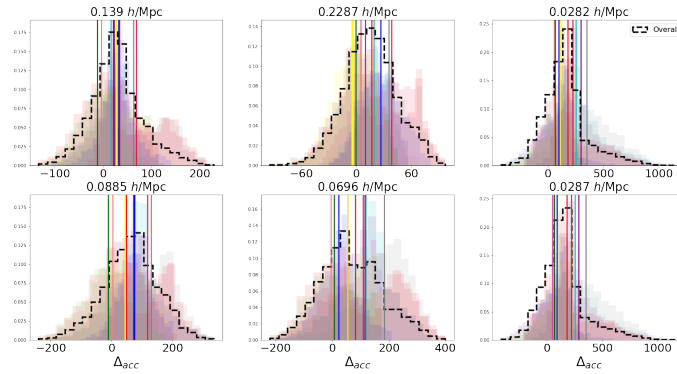


FIG. 9.—: As Fig. (8) but for the accurate neural net, with the same conclusion.

APPENDIX

APPENDIX A

Our neural nets are validated over a 10000 points validation set, which is also used to compute $\bar{\Delta}$ and Σ that define our new posterior. Fig. 6 and Fig. 7 show the performance of the models on the validation set. Each point in parameter space displays the average error over all wavenumbers.

As can be seen, the accurate net mainly produces 3% average error with a few points going up to 6%. On the other hand, the bulk of the points for the inaccurate model reach 30% errors.

APPENDIX B

In order to further validate our assumption that $\mathcal{D}(\Delta)$ is Gaussian and constant throughout parameter space, we do a sub-volume analysis of this distribution. By sub-volume we imply small regions of the parameter space, where we study if gaussianity also holds and if the mean Δ in these sub-volumes falls well within the bulk in the general $\mathcal{D}(\Delta)$ distribution. In Fig. 8 and Fig. 9 we see that most of the sub-volume means fall into the 2σ region and this holds for both the accurate and the inaccurate neural net. Hence, $\mathcal{D}(\Delta)$ does not depend on cosmological parameters which fulfills our assumption.

We further tested in each subvolume the assumption of Gaussianity by computing the skewness and kurtosis and found that Gaussianity is verified with sufficient accuracy. In particular, there were no bimodal distributions for Δ , which would most quickly invalidate the approximation of Δ being Gaussianly distributed.

REFERENCES

Boruah S. S., Eifler T., Miranda V., M S. K. P., 2022, arXiv e-prints, p. [arXiv:2203.06124](https://arxiv.org/abs/2203.06124)
 LSST Science Collaboration et al., 2009, arXiv e-prints, p. [arXiv:0912.0201](https://arxiv.org/abs/0912.0201)
 Laureijs R., et al., 2011, arXiv e-prints, p. [arXiv:1110.3193](https://arxiv.org/abs/1110.3193)
 Lewis A., Bridle S., 2002, *Phys. Rev. D*, 66, 103511
 Manrique-Yus A., Sellentin E., 2020, *MNRAS*, 491, 2655
 Mellema G., et al., 2013, *Experimental Astronomy*, 36, 235

Mootoovaloo A., Heavens A. F., Jaffe A. H., Leclercq F., 2020,
[MNRAS, 497, 2213](#)
Planck Collaboration 2018, arXiv e-prints, p. arXiv:1807.06209
Sellentin E., Heavens A. F., 2016, [MNRAS, 456, L132](#)

This paper was built using the Open Journal of Astrophysics L^AT_EX template. The OJA is a journal which

Spurio Mancini A., Piras D., Alsing J., Joachimi B., Hobson
M. P., 2022, [MNRAS, 511, 1771](#)
de Mijolla D., Viti S., Holdship J., Manolopoulou I., Yates J.,
2019, [A&A, 630, A117](#)

provides fast and easy peer review for new papers in the **astro-ph** section of the arXiv, making the reviewing process simpler for authors and referees alike. Learn more at <http://astro.theoj.org>.